

Critical properties of the Baxter-Wu model on the Union-Jack lattice

Chengxiang Ding¹, Yancheng Wang², and Wanzhou Zhang³

¹*Applied Physics Department, Anhui University of Technology, Maanshan 243002, People's Republic of China*

²*Physics Department, Beijing Normal University,*

Beijing 100875, People's Republic of China and

³*College of Physics and Optoelectronics, Taiyuan University of Technology, Shanxi 030024, People's Republic of China*

(Dated: August 1, 2012)

As a generalization of the Baxter-Wu model, we numerically study the Ising model with triplet interactions on the Union-Jack lattice, which we call as Union-Jack Baxter-Wu model. By means of finite-size scaling analysis based on Monte Carlo simulations and transfer matrix calculations, we numerically determine the critical exponents (or scaling dimensions) and the central charge of the model. The critical exponents studied include y_t , y_h , y_{h1} , and y_{h2} , where y_t governs the critical behavior of the correlation length, y_h governs the critical behavior of the magnetization of the whole lattice, y_{h1} and y_{h2} govern respectively the critical behaviors of the magnetizations on the two sublattices of the Union-Jack lattice. For the critical exponents y_t , y_{h1} , y_{h2} , and the critical points of the model, our numerical estimations coincide with the exact solutions. For the critical exponent y_h and the central charge c , as we know, there is no exact solutions, thus our numerical results are the first determination of these exponents. The exact solutions and our numerical results show that the critical exponent y_{h1} and the central charge c take the same values as those of the 4-state Potts model, which suggests that the model ‘partially’ conserves the critical properties of the 4-state Potts universality.

PACS numbers: 05.50.+q, 64.60.Cn, 64.60.Fr, 75.10.Hk

I. INTRODUCTION

The exact solution[1, 2] of the Ising model significantly promotes the research of phase transition and critical phenomena. After that, the Ising model becomes one of the most famous lattice models in statistical physics. Another famous Ising system, known as the Baxter-Wu model[3], is defined on the triangular lattice. The model has three-spin interactions, and the reduced Hamiltonian is written as

$$-H/k_B T = K \sum_{\langle i,j,k \rangle} s_i s_j s_k, \quad (1)$$

where s_i, s_j, s_k are the Ising spins sitting at the three points of an elementary triangle, and K is the coupling constant of the three spins. The sum takes over all the elementary triangles. This model was firstly proposed by Wood and Griffiths[4] and exactly solved by Baxter and Wu[3] by relating the model with the coloring problem on the honeycomb lattice. The solution gives the critical exponents $y_t = 3/2$ ($\alpha = 2/3$) and $y_h = 15/8$ ($\eta = 1/4$), which are exactly the same as those of the 4-state Potts model[5, 6], which can be derived by the Coulomb gas theory[7]. This means the Baxter-Wu model is in the same universality of the 4-state Potts model. This result can also be understood by the fact that both the Baxter-Wu model and the 4-state Potts model have four-fold degenerate ground state. The critical properties of the 4-state Potts model are affected by the logarithmic corrections[8] because of the second temperature field, which are marginally relevant, however, this is not the case for the Baxter-Wu model. Deng *et al.* generalize the Baxter-Wu model in [9] where the spins are allowed to be q states (q can be larger than 2) and the up- and down-triangles can have different coupling constants. Both generalizations lead to discontinuous phase transitions.

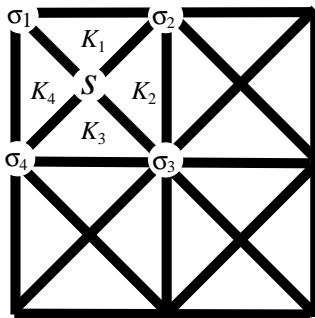


FIG. 1. The Baxter-Wu model on the Union-Jack lattice: the lattice consists of two sublattices, the spin on sublattice A is denoted as σ and the spin on sublattice B is denoted as s ; for a square unit cell, there are four spins $\sigma_1, \sigma_2, \sigma_3$, and σ_4 on sublattice A and one spin s on sublattice B.

In 1972, Hintermann and Merlini[10] considered an Ising system with pure three-spin interactions on the Union-Jack lattice (as shown in Fig. 1)

$$-H/k_B T = \sum_{\{s,\sigma\}} s(K_1\sigma_1\sigma_2 + K_2\sigma_2\sigma_3 + K_3\sigma_3\sigma_4 + K_4\sigma_4\sigma_1), \quad (2)$$

where the sum takes over all the square unit cells and K_i ($i = 1, 2, 3, 4$) are the coupling constants. The model can also be viewed as a generalization of the (triangle) Baxter-Wu model, thus in current paper, we call the model as Union-Jack Baxter-Wu model. For the ferromagnetic case ($K_i > 0$), the model also has four-fold degeneracy of the ground state (as shown in Fig. 2), thus 4-state Potts universality is expected for the model. However, the exact solutions[10, 11] show that the model has critical exponents which change along with the coupling constants.

Through mapping to the eight-vertex model[12, 13], this model can be exactly solved[10], the critical point and critical exponent y_t are obtained. Using the similar method, Wu calculates the spontaneous magnetizations of the model on the two sublattices, the results show that the two magnetizations possess different critical exponents[11].

In current paper, we will numerically study the ferromagnetic Union-Jack Baxter-Wu model for the case with $K_1 = K_3 > 0$ and $K_2 = K_4 > 0$, the numerical procedure includes the Monte Carlo simulations and the transfer matrix calculations. The paper is arranged as follows: In Sec. II, we summarize the results of exact solutions. In Sec. III, we describe the algorithm that we used in Monte Carlo simulations and give the associated numerical results. In Sec. IV, we introduce the transfer matrix calculations and give the associated numerical results. In Sec. V, we summarize the paper and give some discussions.

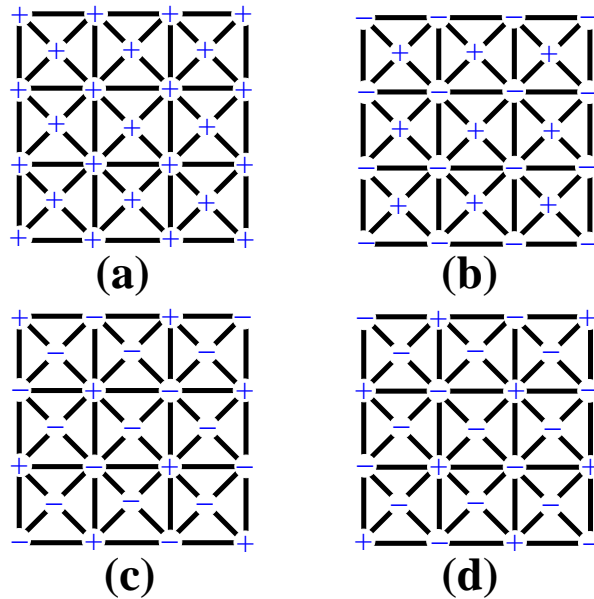


FIG. 2. (Color online) Four ground states of the Union-Jack Baxter-Wu model.

II. EXACT SOLUTIONS

We summarize the results of exact solutions in this section[10, 11].

Assign arrows between the nearest-neighboring Ising spins of sublattice A (Fig. 3): if the two spins besides the arrow is the same, the arrow is rightward (or upward), otherwise it is leftward (or downward). There is a two-to-one correspondence between the Ising spin configurations and the arrow configurations.

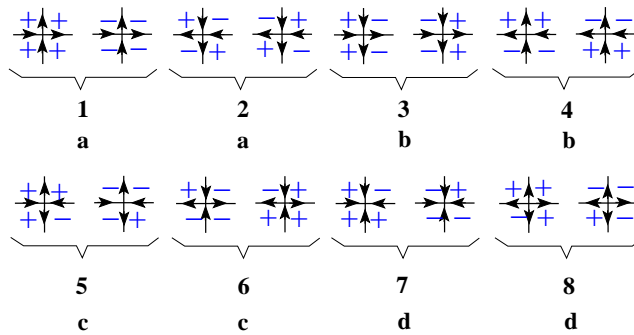


FIG. 3. (Color online) The mapping of the Union-Jack Baxter-Wu model to the eight-vertex model and the Boltzmann weights of the vertexes. The Ising spins shown here are the spins on sublattice A, namely the σ spins.

After taking sum over the spin s (in the center of the unit cell), the Boltzmann weights of the vertexes are

$$\begin{aligned} a &= \cosh(K_1 + K_2 + K_3 + K_4), \\ b &= \cosh(K_1 - K_2 + K_3 - K_4), \\ c &= \cosh(K_1 - K_2 - K_3 + K_4), \\ d &= \cosh(K_1 + K_2 - K_3 - K_4). \end{aligned} \quad (3)$$

Thus the model is mapped to the symmetric eight vertex model[12, 13], which was exactly solved by Baxter. For the ferromagnetic case that we consider in current paper, the critical point is given by

$$a = b + c + d, \quad (4)$$

which gives $K_c = \log(1 + \sqrt{2})/2$ for the uniform case $K = K_1 = K_2 = K_3 = K_4$.

The singularity of the free energy density is governed by

$$f_{\text{sing}} \propto |T - T_c|^{\pi/u} = |T - T_c|^{2/y_t} \quad (5)$$

when $\pi/2u$ is not integer (The case with $\pi/2u = \text{integer}$ is not considered in current paper). $T_c = 1/K_c$ is the critical temperature and $0 \leq u \leq \pi$ is given by [11]

$$\cos u = -\tanh\left[\frac{1}{2}\log\frac{ab}{cd}\right]\Big|_{T_c} \quad \text{if } a > b, c, d, \text{ or } b > a, c, d \quad (6)$$

$$= \tanh\left[\frac{1}{2}\log\frac{ab}{cd}\right]\Big|_{T_c} \quad \text{if } d > a, b, c, \text{ or } c > a, b, d. \quad (7)$$

For the ferromagnetic case that we consider, u is determined by (6). (5) gives the critical exponent

$$y_t = \frac{2u}{\pi}, \quad (8)$$

where y_t also governs the critical behavior of the correlation length: $\xi \sim |T - T_c|^{-1/y_t}$. For the uniform case, (8) gives $y_t = 4/3$.

A very interesting critical property of the Union-Jack Baxter-Wu model is: the spontaneous magnetizations of the two sublattices possess different critical exponents

$$M_A \propto (T_c - T)^{\beta_a}, \quad (9)$$

$$M_B \propto (T_c - T)^{\beta_b}, \quad (10)$$

where M_A and M_B are the magnetizations on sublattice A and B, respectively. The critical exponents β_a and β_b are obtained by Wu[11]

$$\begin{aligned} \beta_a &= \frac{\pi}{16u}, \\ \beta_b &= \frac{\pi - u}{4u}. \end{aligned} \quad (11)$$

Notation: in Eq. (16) of [11], the author reversely writes the critical exponents of M_A and M_B .

According to the scaling law, the magnetic exponents y_{h1} and y_{h2} are

$$\begin{aligned} y_{h1} &= 2 - \beta_a y_t = \frac{15}{8}, \\ y_{h2} &= 2 - \beta_b y_t = \frac{3\pi + u}{2\pi}. \end{aligned} \quad (12)$$

Here y_{h1} has fixed value $15/8$, while y_{h2} varies continuously with the parameters of the model. In the following sections, we will numerically study the critical properties of the Union-Jack Baxter-Wu model, the critical points and critical exponents will be numerically verified. Especially, Wu's results of β_a and β_b (consequently y_{h1} and y_{h2}) are based on the conjectured results of the spontaneous magnetization[14] and spontaneous polarization[15] of the eight-vertex model, thus numerical verification is very necessary.

We are also interested in the critical property of the magnetization of the whole lattice M , whose critical behavior is assume to be governed by a critical exponent β (consequently $y_h = 2 - \beta y_t$)

$$M \propto (T_c - T)^\beta. \quad (13)$$

As we know, the critical exponent y_h (or β) is still neither exactly solved nor numerically determined, we will determine it by Monte Carlo simulations in the next section.

III. MONTE CARLO SIMULATIONS

The triangle Baxter-Wu model has been simulated by the Metropolis algorithm[16], the Wang Landau algorithm[17], and a cluster algorithm[9, 18]. The cluster algorithm[9] is similar to the Swendsen-Wang algorithm[19] for the Potts model. In this algorithm, the triangular lattice is divided as three triangular sublattices. By randomly freezing the spins on one of the sublattices, the other two sublattices compose a honeycomb lattice with pair interactions, then a Swendsen-Wang type algorithm can be formed to update the spins on this honeycomb lattice. For details of this cluster algorithm, see [9]. In current paper, we suitably modify this cluster algorithm to simulate the Union-Jack Baxter-Wu model.

The algorithm is divided into three steps:

1. Step 1, update the spins on sublattice A.

Let the spins on sublattice B be unchanged (frozen) in this step, the interactions of the spins on sublattice A reduce to pair interactions.

A. bonds. Every edge on sublattice A is clamped by two triangles, the interactions of the left and right triangles can be denoted respectively as K_l and K_r , where K_l and K_r may take the values K_1, K_2, K_3 , and K_4 . Place a bond on this edge with probability $p = 1 - e^{-2K_l}$ if only the product of the three spins of the left triangle is 1, $p = 1 - e^{-2K_r}$ if only the product of the right triangle is 1, $p = 1 - e^{-2K_l - 2K_r}$ if both the product of the left triangle and the product of the right triangle are 1, $p = 0$ otherwise.

B. clusters. A cluster is defined as a group of sites on sublattice A connected through the bonds.

C. update spins. Independently flip the spins of each cluster with probability 1/2.

2. Step 2, update the spins on sublattice B and half of the spins on sublattice A.

This step is very similar to step 1, but we freeze only half of the spins on sublattice A, which are labeled A_1 (Fig. 4). The other spins (on sublattice $B+A_2$) are updated, whose interactions also reduce to pair interactions when A_1 spins are frozen.

3. Step 3, update the spins on sublattice B and the other half of the spins on sublattice A.

In this step, the spins labeled A_2 (in Fig. 4) are frozen, other spins (on sublattice $B+A_1$) are updated.

In a complete sweep, all the spins are updated twice.

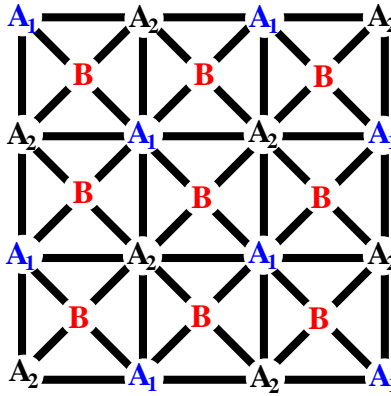


FIG. 4. (Color online) When B spins are frozen, the interactions of A spins (A_1 and A_2 spins) reduce to pair interactions; when A_1 spins are frozen, the interactions of $B + A_2$ spins reduce to pair interactions; when A_2 spins are frozen, the interactions of $B + A_1$ spins reduce to pair interactions.

In the simulations, the sampled variables include the specific heat C , the magnetization of the whole lattice M , the magnetization on sublattice A M_A , and the magnetization on sublattice B M_B . The specific heat is defined by the fluctuation of internal energy

$$C = \frac{1}{L^2} \frac{\langle E^2 \rangle - \langle E \rangle^2}{k_B T^2}, \quad (14)$$

where E is the internal energy, L is the linear size of the system, and $\langle \dots \rangle$ means the ensemble average. The magnetizations are defined as

$$M = \frac{\langle |\sum_{i=1}^N \sigma_i + \sum_{i=1}^N s_i| \rangle}{2N}, \quad (15)$$

$$M_A = \frac{\langle |\sum_{i=1}^N \sigma_i| \rangle}{N}, \quad (16)$$

$$M_B = \frac{\langle |\sum_{i=1}^N s_i| \rangle}{N}, \quad (17)$$

where $N = L^2$ is the total sites on sublattice A or B.

In order to demonstrate our numerical procedure based on the Monte Carlo simulations, we take the uniform case ($K = K_1 = K_2 = K_3 = K_4$) as an example. The cluster algorithm is very efficient, it easily allows us to do meaningful simulations for system with linear size up to $L = 256$. All the simulations are performed at the critical point K_c . After equilibrating the system, 10^7 samples were taken for each system size. Using the Levenberg-Marquardt algorithm, we fit the data of C according to the finite-size scaling formula[20]

$$C(L) = C_0 + L^{2y_t-d}(a + bL^{y_1}), \quad (18)$$

where bL^{y_1} are the leading correction-to-scaling and $y_1 < 0$ is the leading irrelevant exponent. $d = 2$ is the dimension of the lattice. C_0 , a , and b are unknown parameters. The fitting yields $y_t = 1.332(2)$, which is in good agreement with the exact solution $y_t = 4/3$.

Similar procedure was applied to the magnetizations M , M_A , and M_B , according to the finite-size scaling formulas[20]

$$M = L^{y_h-d}(a + bL^{y_1}), \quad (19)$$

$$M_A = L^{y_{h1}-d}(a + bL^{y_1}), \quad (20)$$

$$M_B = L^{y_{h2}-d}(a + bL^{y_1}). \quad (21)$$

The log-log plot of M , M_A , and M_B versus L are shown in Fig. 5. The fitting of the data yield $y_h = 1.857(1)$, $y_{h1} = 1.874(1)$, and $y_{h2} = 1.833(1)$, where y_{h1} and y_{h2} are in good agreement with the exact solutions $y_{h1} = 15/8$ and $y_{h2} = 11/6$, respectively.

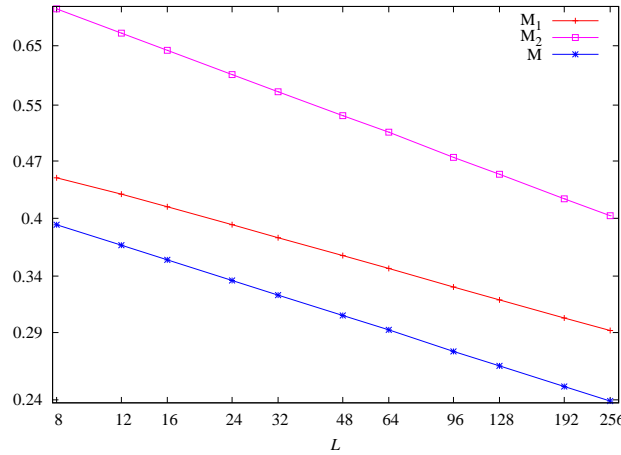


FIG. 5. (Color online) Log-Log plot of the magnetizations (M , M_1 , M_2) versus system size L for the Union-Jack Baxter-Wu model at the critical point $K_c = \log(1 + \sqrt{2})/2$ for the uniform case ($K = K_1 = K_2 = K_3 = K_4$).

We also simulate the cases with $r = K'/K = 1, 2, 3, 4$, and 5 , where $K = K_1 = K_3$ and $K' = K_2 = K_4$. All the exact solutions and numerical estimations are listed in Table I. From the table we can see that the numerical estimations for y_t , y_{h1} , and y_{h2} are in good agreement with the exact solutions. To the best of our knowledge, there is no exact solution for y_h until now, thus our numerical result is the first determination of this critical exponent for the Union-Jack Baxter-Wu model.

IV. TRANSFER MATRIX CALCULATIONS

As shown in Fig. 6, we define the row-to-row transfer matrix

$$\begin{aligned} T_{\vec{\sigma}, \vec{\sigma}'} &= \sum_{\{s_1, s_2, \dots, s_L\}} \prod_{i=1}^L \exp[s_i(K_1\sigma_i\sigma_{i+1} + K_2\sigma_{i+1}\sigma'_{i+1} + K_3\sigma'_{i+1}\sigma'_i + K_4\sigma'_i\sigma_i)] \\ &= 2^L \prod_{i=1}^L \cosh(K_1\sigma_i\sigma_{i+1} + K_2\sigma_{i+1}\sigma'_{i+1} + K_3\sigma'_{i+1}\sigma'_i + K_4\sigma'_i\sigma_i), \end{aligned} \quad (22)$$

TABLE I. Critical points, critical exponents, and scaling dimensions of the Union-Jack Baxter-Wu model. $r = K'/K$, where $K = K_1 = K_3$ and $K' = K_2 = K_4$. E=Exact result, MC=Numerical result based on Monte Carlo simulations. TM=Numerical result based on transfer matrix calculations. The critical exponents and the scaling dimensions are related by $y_t = 2 - X_t$, $y_{h1} = 2 - X_{h1}$, and $y_{h2} = 2 - X_{h2}$.

| r | | 1 | 2 | 3 | 4 | 5 |
|----------|----|---------------|--------------|--------------|--------------|--------------|
| K_c | E | 0.4406867935 | 0.3046889317 | 0.2406059125 | 0.2017629641 | 0.1751991102 |
| | TM | 0.44068679(5) | 0.3046889(1) | 0.2406059(1) | 0.2017629(1) | 0.1751991(2) |
| y_t | E | 4/3 | 1.39668184 | 1.47604048 | 1.53960311 | 1.58921160 |
| | MC | 1.332(2) | 1.397(4) | 1.478(4) | 1.540(3) | 1.590(4) |
| X_t | E | 2/3 | 0.60331816 | 0.52395952 | 0.46039689 | 0.41078840 |
| | TM | 0.66666(1) | 0.603318(1) | 0.52396(1) | 0.46040(2) | 0.41079(1) |
| y_{h1} | E | 15/8 | 15/8 | 15/8 | 15/8 | 15/8 |
| | MC | 1.874(1) | 1.874(2) | 1.876(2) | 1.877(3) | 1.873(4) |
| X_{h1} | E | 1/8 | 1/8 | 1/8 | 1/8 | 1/8 |
| | TM | 0.125000(1) | 0.125000(1) | 0.125000(1) | 0.12500(1) | 0.12498(3) |
| y_{h2} | E | 11/6 | 1.84917046 | 1.86901012 | 1.88490078 | 1.89730290 |
| | MC | 1.833(1) | 1.848(2) | 1.870(2) | 1.886(3) | 1.896(4) |
| X_{h2} | E | 1/6 | 0.15082954 | 0.13098988 | 0.11509922 | 0.10269710 |
| | TM | 0.166666(1) | 0.150829(1) | 0.130990(1) | 0.115099(1) | 0.102696(2) |
| y_h | E | - | - | - | - | - |
| | MC | 1.855(2) | 1.862(3) | 1.874(3) | 1.882(4) | 1.888(4) |
| c | E | 1 | 1 | 1 | 1 | 1 |
| | MC | 1.000000(1) | 1.000000(1) | 0.99998(3) | 1.0000(2) | 0.9999(1) |

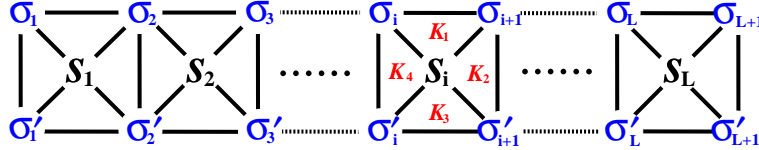


FIG. 6. (Color online) Definition of the row-to-row transfer matrix, where periodic boundary conditions are applied, namely $\sigma_{L+1} = \sigma_1$, $\sigma'_{L+1} = \sigma'_1$.

where $\vec{\sigma} = (\sigma_1, \sigma_2, \dots, \sigma_L)$ and $\vec{\sigma}' = (\sigma'_1, \sigma'_2, \dots, \sigma'_L)$ are the states of two neighboring rows. In the definition, periodic boundary conditions are applied, namely $\sigma_{L+1} = \sigma_1$ and $\sigma'_{L+1} = \sigma'_1$. For a system with M rows, the partition sum is

$$\begin{aligned}
 Z &= \sum_{\{\vec{\sigma}_1, \vec{\sigma}_2, \dots, \vec{\sigma}_M\}} T_{\vec{\sigma}_1, \vec{\sigma}_2} T_{\vec{\sigma}_2, \vec{\sigma}_3} \cdots T_{\vec{\sigma}_M, \vec{\sigma}_{M+1}} \\
 &= \sum_{\{\vec{\sigma}_1, \vec{\sigma}_2, \dots, \vec{\sigma}_M\}} T_{\vec{\sigma}_1, \vec{\sigma}_2} T_{\vec{\sigma}_2, \vec{\sigma}_3} \cdots T_{\vec{\sigma}_M, \vec{\sigma}_1} \\
 &= \sum_{\vec{\sigma}_1} (T \cdot T \cdots T)_{\vec{\sigma}_1, \vec{\sigma}_1} \\
 &= \text{Trace}(T^M),
 \end{aligned} \tag{23}$$

where $\vec{\sigma}_i$ is the state of the i -th row and periodic boundary conditions are also applied, namely $\vec{\sigma}_{M+1} = \vec{\sigma}_1$. In the limit $M \rightarrow \infty$, the free energy density is given by

$$\begin{aligned}
 f &= \lim_{M \rightarrow \infty} \frac{1}{ML} \log \text{Trace}(T^M) \\
 &= \lim_{M \rightarrow \infty} \frac{1}{ML} \log(\Lambda_1^M + \Lambda_2^M + \Lambda_3^M \cdots) \\
 &= \frac{1}{L} \log \Lambda_1,
 \end{aligned} \tag{24}$$

where $\Lambda_1, \Lambda_2, \Lambda_3, \dots$ are the eigenvalues of T , with $\Lambda_1 \geq \Lambda_2 \geq \Lambda_3 \cdots$. An exact solution of Λ_1 determines the free energy density of the system. Furthermore, not only the free energy density, but also some critical exponents are also determined by the eigenvalues of the transfer matrix, which will be shown concretely bellow.

To numerically calculate some of the eigenvalues of the matrix, the sparse matrix technique is very useful, it sharply reduce the requirement of computer memory for storing the matrix elements. For detailed study of this technique, see [21–24]. For the Union-Jack Baxter-Wu model, the dimension of the matrix T is $d_T = 2^L$. By using the technique of sparse matrix decomposition, we are able to calculate the eigenvalues of T with L up to 22. In order to obtain meaningful eigenvalues, the L must be even because of the symmetry of the ordered phase, as shown by Fig. 2, especially by Fig. 2(c) and (d). For a finite system, the symmetry can be conserved only if the size is even.

In order to study the critical properties of the Union-Jack Baxter-Wu model, we calculate the scaled gap $X(K, L)$, which is generally defined as

$$X(K, L) = \frac{1}{2\pi} \log \left(\frac{\Lambda_1}{\Lambda_i} \right), \quad (25)$$

where Λ_1 and Λ_i are the leading and the other eigenvalues of the matrix T , respectively. According to the conformal invariance theory[25], the scaled gap $X(K, L)$ is related with the correlation length $\xi(K, L)$ with

$$X(K, L) = \frac{L}{2\pi\xi(K, L)}, \quad (26)$$

where $\xi(K, L)$ governs the decay of the correlation function $G(r)$:

$$G(r) \propto e^{-r/\xi(K, L)}. \quad (27)$$

The correlation function $G(r)$ can be energy correlation or magnetic correlation. For example, the magnetic correlation function can be defined as $G(r) = \langle s_0 s_r \rangle$ or the probability of two spins with distance r have the same value. For the Union-Jack Baxter-Wu model, because we are interested in the different critical properties of the two sublattices, we can define other types of magnetic correlation functions, where we confine s_0 and s_r on one of the sublattices. For clarity, we let $G(r)$ represent the magnetic correlation function on the whole lattice, let $G_A(r)$ and $G_B(r)$ represent respectively the magnetic correlation functions on the A and B sublattices. We further express the scaled gaps corresponding to $G(r)$, $G_A(r)$, $G_B(r)$ as $X_h(K, L)$, $X_{h1}(K, L)$, $X_{h2}(K, L)$, respectively, and express the scaled gap corresponding to the energy correlation function as $X_t(K, L)$.

In the procedure of transfer matrix calculations, we find that, the scaled gaps are determined by the first four eigenvalues as (25). The concrete order are determined by the magnitude of the gaps. For example, when $X_{h1} < X_{h2} < X_t$, the scaled gap $X_{h1}(K, L)$ is determined by eigenvalues Λ_1 and Λ_2 , $X_{h2}(K, L)$ is determined by Λ_1 and Λ_3 , and $X_t(K, L)$ is determined by Λ_1 and Λ_4 :

$$\begin{aligned} X_{h1}(K, L) &= \frac{L}{2\pi} \log \frac{\Lambda_1}{\Lambda_2}, \\ X_{h2}(K, L) &= \frac{L}{2\pi} \log \frac{\Lambda_1}{\Lambda_3}, \\ X_t(K, L) &= \frac{L}{2\pi} \log \frac{\Lambda_1}{\Lambda_4}, \end{aligned} \quad (28)$$

however, when $X_{h2} < X_{h1} < X_t$, the gaps are determined by

$$\begin{aligned} X_{h1}(K, L) &= \frac{L}{2\pi} \log \frac{\Lambda_1}{\Lambda_3}, \\ X_{h2}(K, L) &= \frac{L}{2\pi} \log \frac{\Lambda_1}{\Lambda_2}, \\ X_t(K, L) &= \frac{L}{2\pi} \log \frac{\Lambda_1}{\Lambda_4}, \end{aligned} \quad (29)$$

and so forth.

Unfortunately, we are unable to find which eigenvalues determine $X_h(K, L)$.

According to the finite-size scaling[20] and the conformal invariance[25], the scaled gaps X_{h1} and X_{h2} in the vicinity of the critical point K_c satisfy

$$X_{h1}(K, L) = X_{h1} + a(K - K_c)L^{y_t} + buL^{y_u} + \dots, \quad (30)$$

$$X_{h2}(K, L) = X_{h2} + a'(K - K_c)L^{y_t} + b'uL^{y_u} + \dots, \quad (31)$$

where X_{h1} and X_{h2} are the scaling dimensions. u is the irrelevant field, and $y_u < 0$ is the associated irrelevant exponent. a, a', b , and b' are unknown constants. Fig. 7 and Fig. 8 are illustrations of $X_{h1}(K, L)$ and $X_{h2}(K, L)$ versus K respectively, for the uniform case.

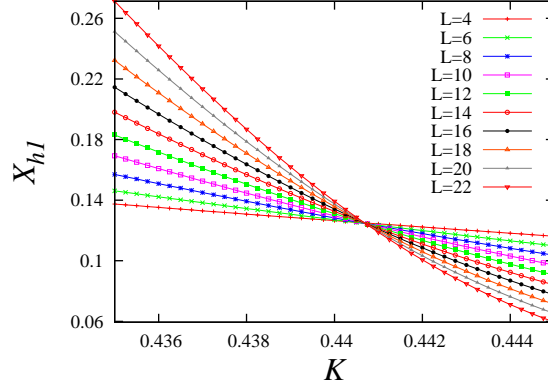


FIG. 7. (Color online) Scaled gap $X_{h1}(K, L)$ versus K for a sequence of system size L for the uniform Union-Jack Baxter Wu model ($r = 1$), whose critical point is $K_c = \log(1 + \sqrt{2})/2 = 0.440687$.

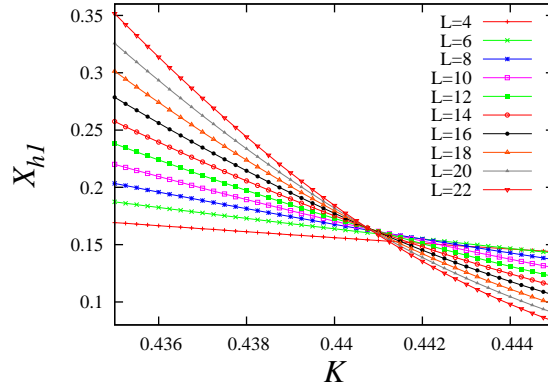


FIG. 8. (Color online) Scaled gap $X_{h2}(K, L)$ versus K for a sequence of system size L for the uniform Union-Jack Baxter Wu model ($r = 1$), whose critical point is $K_c = \log(1 + \sqrt{2})/2 = 0.440687$.

We numerically solve the finite-size scaling equation

$$X_{h1}(K, L) = X_{h1}(K, L - 1), \quad (32)$$

or

$$X_{h2}(K, L) = X_{h2}(K, L - 1), \quad (33)$$

and denote the solution by $K_c(L)$, which satisfies

$$K_c(L) = K_c + auL^{y_u - y_t} + \dots \quad (34)$$

Here a are unknown constant. $y_u < 0$ and $y_t \geq 0$, thus $K_c(L)$ converges to the critical point K_c for increasing system size. (34) is used to determine the critical point in our numerical procedure. For the uniform case ($r = 1$), it gives $K_c = 0.44068679(5)$, which is in good agreement with the exact solution $K_c = \log(1 + \sqrt{2})/2$. We have also estimated the critical points of the cases with $r = 2, 3, 4$, and 5 , all of our numerical estimations of K_c , which are consistent with the exact solutions in a high accuracy, are listed in Table I. Sincerely, both (30) and (31) can be used to estimate the critical points, in Table I we list the best estimations.

Exactly at the critical point K_c , (30) and (31) reduces to

$$X_{h1}(L) = X_{h1} + buL^{y_u} + \dots, \quad (35)$$

$$X_{h2}(L) = X_{h2} + b'uL^{y_u} + \dots \quad (36)$$

These equations are used to determine the scaling dimensions X_{h1} and X_{h2} in our numerical procedure. For the uniform case, it gives $X_{h1} = 0.125000(1)$, and $X_{h2} = 0.166666(1)$, which are consistent with the exact solutions (Table I). We also applied the same procedure to the other cases, the numerical estimations and exact solutions are listed in Table I.

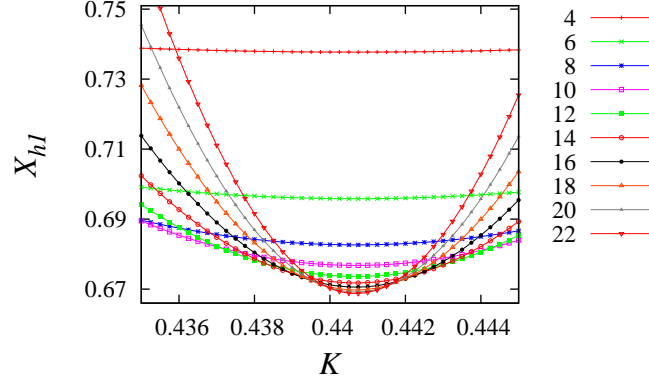


FIG. 9. (Color online) Scaled gap $X_t(K, L)$ versus K for a sequence of system size L for the uniform Union-Jack Baxter Wu model ($r = 1$), whose critical point is $K_c = \log(1 + \sqrt{2})/2 = 0.440687$.

We also calculate the scaled gap $X_t(K, L)$, its critical behavior seems somewhat different from that of X_{h1} or X_{h2} . This is shown in Fig. 9 for the uniform case. The lowest point of the line for a given L can be denoted as $(K_c(L), X_t(K_c(L), L))$, and the value of $K_c(L)$ seems to converge to the critical point K_c for increasing L . This property can also be used to estimate K_c , for examples, see [26]. But we haven't do this in current paper, because we have estimated K_c by the critical behavior of X_{h1} or X_{h2} . However, exactly at the critical point K_c , the value of $X_t(K_c, L)$ seems to satisfy the formula

$$X_t(K_c, L) = X_t + buL^{y_u} + \dots, \quad (37)$$

which is very similar to (35) or (36). We use (37) to estimate the scaling dimension X_t in our numerical procedure, the results are also listed in Table I.

The scaling dimensions X_{h1} , X_{h2} , and X_t are related with the critical exponents by[25]

$$\begin{aligned} y_{h1} &= 2 - X_{h1}, \\ y_{h2} &= 2 - X_{h2}, \\ y_t &= 2 - X_t. \end{aligned} \quad (38)$$

This allows us to compare the results of the transfer matrix calculations, the Monte Carlo simulations, and the exact solutions (Table I).

According to the finite-size scaling[20] and the conformal invariance[25], the free energy density scales as

$$f(L) \simeq f(\infty) + \frac{\pi c}{6L^2} \quad (39)$$

at the critical point, where c is the central charge in the conformal theory[25]. Fitting the data of the free energy density according to (39), we get the central charge $c = 1.000000(1)$ for the uniform case. For the other cases, the numerical estimations of the central charge are also listed in Table I. As we know, this is the first determination of the central charge of the Union-Jack Baxter-Wu model. It seems that the central charge takes the fixed value $c = 1$, which is the same as that of the 4-state Potts model.

V. CONCLUSION AND DISCUSSIONS

In conclusion, we have numerically studied the critical properties of the Union-Jack Baxter-Wu model, by means of finite-size scaling analysis based on the Monte Carlo simulations and the transfer matrix calculations. For the critical points and critical exponents y_t (X_t), y_{h1} (X_{h1}), and y_{h2} (X_{h2}), our numerical estimations are in good agreement with the exact solutions[10, 11]. To the best of our knowledge, there is no exact solutions of the critical exponents y_h and the central charge c , thus our numerical results are the first determination of these exponents. The numerical results show that y_h varies continuously with the parameters of the model, while the central charge seems to take the fixed value $c = 1$, which is the same as that of the 4-state Potts model.

The ground state of the (ferromagnetic) Union-Jack Baxter-Wu model is four-fold degenerate, thus the phase transition of the model is expected to be in the universality of the 4-state Potts model. However, the model has much more complicated critical properties than the 4-state Potts model, which are shown by the continuous change

of the critical exponents (y_t , y_h , and y_{h2}), and by the difference of the critical exponents on the two sublattices (y_{h1} and y_{h2}).

It seems that the model ‘partially’ conserves the critical properties of 4-state Potts universality, which are shown by the critical exponents y_{h1} and the central charge c , whose values are fixed and the same as those of the 4-state Potts model.

The critical properties of the 4-state Potts model are affected by the logarithmic corrections[8], however, in our numerical procedure, all the data are well fit without the logarithmic correction.

ACKNOWLEDGMENT

We thank Professor F. Y. Wu for valuable discussions. This work is supported by the National Science Foundation of China (NSFC) under Grant No. 11175018, and by the High Performance Scientific Computing Center (HSCC) of Beijing Normal University.

-
- [1] L. Onsager, Phys. Rev. **65**, 117 (1944).
 - [2] C. N. Yang, Phys. Rev. **85**, 808 (1952).
 - [3] R. J. Baxter and F. Y. Wu, Phys. Rev. Lett. **31**, 1294 (1973).
 - [4] D. W. Wood and H. P. Griffiths, J. Phys. C **5**, L253 (1972).
 - [5] R. B. Potts, Proc. Camb. Phys. Soc. **48**, 106 (1952).
 - [6] F. Y. Wu, Rev. Mod. Phys. **54**, 235 (1982).
 - [7] B. Nienhuis, J. Stat. Phys. **34**, 731 (1984).
 - [8] J. Salas and A. D. Sokal, J. Stat. Phys. **88**, 567 (1997).
 - [9] Y. Deng, W.-A. Guo, J. R. Heringa, H. W. J. Blöte, and B. Nienhuis, Nucl. Phys. B **827**[FS], 406 (2010).
 - [10] A. Hintermann and D. Merlini, Phys. Lett. A, **41**, 208 (1972).
 - [11] F. Y. Wu, J. Phys. C **8**, 2262 (1975).
 - [12] R. J. Baxter, Phys. Rev. Lett. **26**, 832 (1971).
 - [13] R. J. Baxter, *Exactly Solved Models in Statistical Mechanics* (Academic, London, 1982).
 - [14] M. N. Barber and R. J. Baxter, J. Phys. C **6**, 2913 (1973).
 - [15] R. J. Baxter and S. B. Kelland, J. Phys. C **7**, L403 (1974).
 - [16] L. N. Shchur and W. Janke, arXiv:1007.1838.
 - [17] N. Schreiber and J. Adler, J. Phys. A **38**, 7253 (2005).
 - [18] H. W. J. Blöte, J. R. Heringa, and E. Luijten, Comp. Phys. Comm. **147**, 58 (2002).
 - [19] R. H. Swendsen and J. S. Wang, Phys. Rev. Lett. **58**, 86 (1987).
 - [20] For reviews, see e.g. M. P. Nightingale in *Finite-Size Scaling and Numerical Simulation of Statistical Systems*, ed. V. Privman (World Scientific, Singapore 1990), and M. N. Barber in *Phase Transitions and Critical Phenomena*, Vol. 8, eds. C. Domb and J. L. Lebowitz (Academic, New York 1983).
 - [21] H. W. J. Blöte and M. P. Nightingale, Physica A (Amsterdam) **112**, 405 (1982).
 - [22] H. W. J. Blöte and B. Nienhuis, J. Phys. A **22**, 1415 (1989).
 - [23] H. W. J. Blöte and M. P. Nightingale, Phys. Rev. B **47**, 15046 (1993).
 - [24] X. F. Qian, M. Wegewijs, and H. W. J. Blöte, Phys. Rev. E **69**, 036127 (2004).
 - [25] J. L. Cardy, in *Phase Transitions and Critical Phenomena*, edited by C. Domb and J. L. Lebowitz (Academic Press, London, 1987), Vol. 11, p. 55, and references therein.
 - [26] H. W. J. Blöte, M. P. Nightingale, Physica A (Amsterdam) **129**, 1 (1984).